

# Time domain reflectometry (TDR) potential for soil condition monitoring of geotechnical assets

Giulio Curioni, David N. Chapman, Alexander C.D. Royal, Nicole Metje, Ben Dashwood, David A. Gunn, Cornelia M. Inauen, Jonathan E. Chambers, Philip I. Meldrum, Paul B. Wilkinson, Russell T. Swift, and Helen J. Reeves

**Abstract:** The performance of geotechnical assets is influenced by various external factors including time and changing loading and environmental conditions. These changes could reduce the asset's ability to maintain its function, potentially resulting in failure, which could be extremely disruptive and expensive to remediate; thus, the ability to monitor the long-term condition of the ground is clearly desirable as this could function as an early-warning system, permitting intervention prior to failure. This study demonstrates, for the first time, the potential of using time domain reflectometry (TDR) for long-term monitoring of the relative health of an asset (via water content and dry density) in a field trial where a clayey sandy silt was exposed to leaking water from a pipe. TDR sensors were able to provide detailed information on the variation in the soil conditions and detect abrupt changes that would relay a prompt for asset inspections or interventions. It is proposed that TDR could be used alone or together with other shallow geophysical techniques for long-term condition monitoring of critical geotechnical assets. Early-warning systems could be based on thresholds defined from the values or the relative change of the measured parameters.

*Key words:* time domain reflectometry, soil condition monitoring, gravimetric water content, dry density, degree of saturation.

**Résumé :** La performance des actifs géotechniques est influencée par divers facteurs externes, notamment le temps et les conditions changeantes de chargement et d'environnement. Ces modifications pourraient réduire la capacité de l'actif à conserver sa fonction, ce qui pourrait entraîner une défaillance qui pourrait être extrêmement perturbatrice et coûteuse à résoudre; ainsi, la capacité de surveiller l'état à long terme du sol est clairement souhaitable, car cela pourrait fonctionner comme un système d'alerte rapide, permettant une intervention avant la panne. Cette étude démontre, pour la première fois, la possibilité d'utiliser la réflectométrie temporelle (TDR) pour surveiller à long terme la santé relative d'un actif dans un essai sur le terrain (via la teneur en eau et la densité sèche) où un silt sableux argileux était exposé à des fuites d'eau. Les capteurs TDR ont été en mesure de fournir des informations détaillées sur la variation des conditions du sol et de détecter les changements brusques qui entraîneraient des inspections ou des interventions sur les actifs. Il est proposé que le TDR puisse être utilisé seul ou conjointement avec d'autres techniques géophysiques peu profondes pour la surveillance de la situation à long terme des actifs géotechniques critiques. Les systèmes d'alerte précoce pourraient être basés sur des seuils définis à partir des valeurs ou de la variation relative des paramètres mesurés. [Traduit par la Rédaction]

*Mots-clés :* réflectométrie temporelle, surveillance de l'état du sol, teneur en eau gravimétrique, densité sèche, degré de saturation.

## Introduction

Modern, developed societies are fundamentally dependent upon the performance of their geotechnical assets (e.g., embankments, cuttings, earth dams, flood levees, pavement subbase layers) to function properly; yet, many of these earth structures and the infrastructure that they support (e.g., transport infrastructure, buried pipes and cables) have been constructed decades, if not centuries, ago and as such are still being relied upon well past their design life (Glendinning et al. 2015; Janik et al. 2017). Replacement of these assets is often prohibitively expensive (Rosenbalm and Zapata 2017); hence, effective management strategies are required to ensure prolonged function. Failure, or situations that threaten the failure, of the geotechnical assets could result in significant damage and (or) disruption to surrounding infrastructure—

facilities (roads, rail, buried pipes, urbanized conurbations, etc.) and society's functions (loss of, or reduction in, service provision) (Du et al. 2016; Clarke et al. 2017).

In addition, increasing population and climate variability are applying unheralded pressures on these aging assets and this is likely to have a negative impact on continued, uninterrupted provision of services (Davies et al. 2008; Jaroszowski et al. 2014; Pritchard et al. 2014, 2015a).

Deterioration, and failure mechanisms, of ageing geotechnical infrastructure have been attributed to a number of processes often related to changes in water content (including rapid-drawdown post-flooding, shrink–swell and desiccation, internal and surface erosion, as well as changes in pore-water pressure and (or) chemistry regimes) (Clayton et al. 2010; Farewell et al. 2012; Rajeev et al. 2012; Glendinning et al. 2014; Pritchard et al. 2014,

Received 27 October 2017. Accepted 13 June 2018.

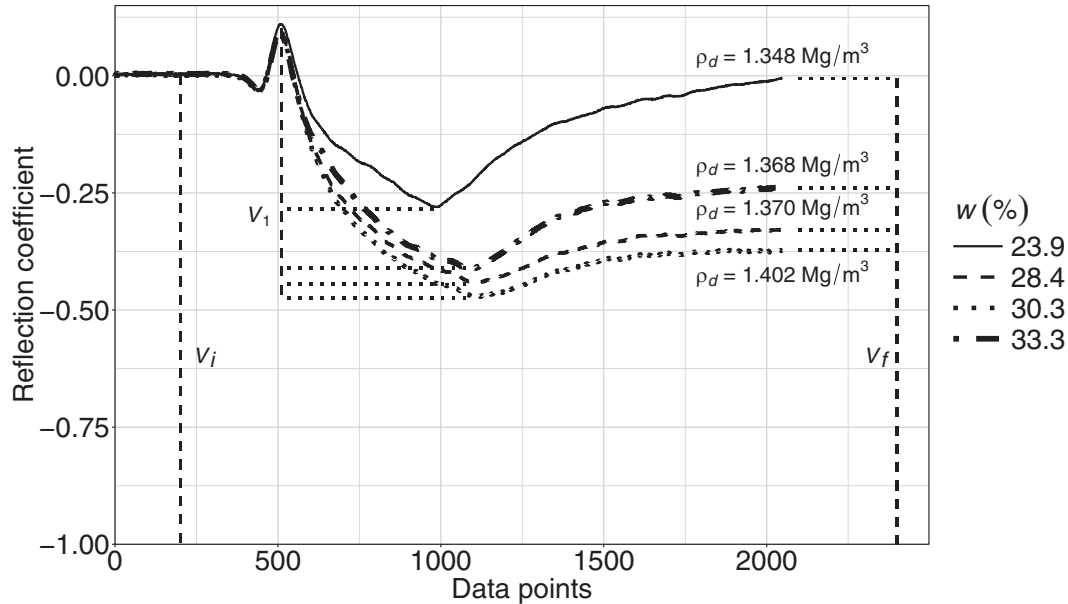
**G. Curioni, D.N. Chapman, A.C.D. Royal, and N. Metje.** Department of Civil Engineering, School of Engineering, University of Birmingham, Edgbaston, Birmingham, B15 2TT, UK.

**B. Dashwood, D.A. Gunn, C.M. Inauen, J.E. Chambers, P.I. Meldrum, P.B. Wilkinson, R.T. Swift, and H.J. Reeves.** British Geological Survey, Environmental Science Centre, Nicker Hill, Keyworth, Nottingham, NG12 5GG, UK.

**Corresponding author:** Giulio Curioni (emails: [g.curioni@bham.ac.uk](mailto:g.curioni@bham.ac.uk), [giulio.curioni@gmail.com](mailto:giulio.curioni@gmail.com)).

Copyright remains with the author(s) or their institution(s). This work is licensed under a [Creative Commons Attribution 4.0 International License](https://creativecommons.org/licenses/by/4.0/) (CC BY 4.0), which permits unrestricted use, distribution, and reproduction in any medium, provided the original author(s) and source are credited.

Fig. 1. Example of TDR waveforms taken in a clayey sandy silt at different values of  $w$  and  $\rho_d$ .  $V_i$ , input voltage.



2015a, 2015b; Rosenbalm and Zapata 2017; Briggs et al. 2017; Janik et al. 2017; Stirling et al. 2017). Hence, it is clear that water content is a key parameter influencing the performance of geotechnical assets.

The soil water content can be expressed on a gravimetric basis ( $w$ ) or on a volumetric basis ( $\theta$ ); while the volumetric water content is used in many disciplines, it is the gravimetric variant that is commonly used in geotechnical engineering and many fundamental indices and relationships in soil mechanics are based on this quantity (e.g., liquid limit, LL, and plastic limit, PL). Electromagnetic (EM) techniques have been widely used for measuring  $\theta$  (Robinson et al. 2008). Among these, time domain reflectometry (TDR) is a well-established method that has been used to measure  $\theta$  and electrical parameters at point locations in the field based on the measurement of the apparent dielectric permittivity,  $K_a$  (Herkelrath et al. 1991; Robinson et al. 2003a; Delin and Herkelrath 2005; Curioni et al. 2017).

TDR has recently been used to monitor earth structures such as levees in controlled experiments and in real field case studies (Scheuermann et al. 2009; Utili et al. 2015; Janik et al. 2017). Estimating the degree of saturation ( $S_r$ ) would be very beneficial as this parameter is directly linked to the stability of earth structures and could be used to trigger warnings (Valentino et al. 2011). Measuring the soil parameters remotely from buried sensors would clearly be advantageous and reduce the current reliance on the visual qualitative inspections conducted by inspection engineers (Utili et al. 2015). Studies using electrical resistivity tomography (ERT) have shown the potential of using  $\theta$  and  $S_r$  for monitoring the condition of ageing embankments and have suggested that these parameters can be used for a more effective management of geotechnical assets (Chambers et al. 2014; Gunn et al. 2015). Warnings could be triggered based on levels of water content with respect to the soil's Atterberg limits (i.e., PL and LL) and relay a prompt for inspections or interventions. It is apparent that measuring  $w$  directly would be particularly convenient if indices such as PL and LL are to be used in early-warning systems because these are defined on a gravimetric basis. If the soil dry density ( $\rho_d$ ) is also known, it could be used together with  $w$  to measure  $S_r$  and a wide range of soil geotechnical properties (e.g., porosity, voids ratio, air content) (BSI 1999b).

Previous studies showed the potential of measuring both  $w$  and  $\rho_d$  with TDR (Siddiqui and Drnevich 1995; Lin et al. 2000; Siddiqui

et al. 2000; Yu and Drnevich 2004; Drnevich et al. 2005; Thring et al. 2014; Jung et al. 2013a, 2013b; Curioni et al. 2018), but these methods have not been tested in field monitoring applications. Recently, Bhuyan et al. (2017) reported an interesting application of the TDR method for monitoring the condition of granular pavement materials. The aim of this paper is to demonstrate the potential use of TDR for soil condition monitoring from the measurement of  $w$  and  $\rho_d$  in a field case study. A clayey sandy silt of high plasticity was flooded a number of times during controlled pipe leak experiments designed to achieve saturation conditions with TDR monitoring the changes induced and the movement of water.

### Proposed TDR method for soil condition monitoring

TDR has been used for some time in geotechnical engineering for compaction quality control based on the measurement of both  $w$  and  $\rho_d$  (Siddiqui and Drnevich 1995; Lin et al. 2000; Siddiqui et al. 2000; Yu and Drnevich 2004; Drnevich et al. 2005). These works led to the development of ASTM standards that have been updated over time to account for new findings and improvements (ASTM 2003, 2005). Following reports of satisfactory and unsatisfactory results (Lin et al. 2012), a new empirical calibration procedure less dependent on compactive effort has been developed by Jung et al. (2013a, 2013b) and forms the basis of the current ASTM D6780/D6780M standard (ASTM 2012). The method consists of an empirical soil-specific calibration conducted using TDR during a standard compaction test (BSI 1999a). Two empirical equations are used in combination and allow the measurement of both  $w$  and  $\rho_d$  from an analysis of the TDR waveforms (eqs. (1) and (2); Fig. 1).

$$(1) \quad \sqrt{K_a \frac{\rho_w}{\rho_d}} = a_1 + b_1 w$$

$$(2) \quad V_r \frac{\rho_w}{\rho_d} = c_1 + d_1 (K_a - 1) - c_1 e^{-f_1 (K_a - 1)}$$

where  $V_r$  is the ratio between the first voltage drop  $V_1$  and the final voltage  $V_f$  as shown in Fig. 1;  $\rho_w$  is the density of water (1 Mg/m<sup>3</sup>); and  $a_1$ ,  $b_1$ ,  $c_1$ ,  $d_1$ , and  $f_1$  are soil-specific coefficients. Figure 1 shows an example of waveforms taken in a clayey sandy silt displaying

the variation of  $V_1$  and  $V_f$  at varying  $\rho_d$  and  $w$ . Jung et al. (2013b) investigated the effect of temperature on the parameters extracted from TDR waveform analysis. They found that the effect on  $K_a$  was limited in the typical range of temperatures found in the field while  $V_1$  and  $V_f$  (and therefore  $V_r$ ) were more significantly affected and had to be corrected. The authors proposed simple empirical corrections designed for either fine-grained or coarse-grained soils.

This method appeals to geotechnical engineers because the standard compaction test is routinely performed and engineers are more familiar with soil water contents expressed as  $w$  rather than  $\theta$ . However, in the original method a specially designed TDR probe was used that has been optimized for reliability and ease of insertion and therefore was well suited for compaction quality control. To use TDR sensors for long-term soil condition monitoring, commercial three-rod TDR probes would be preferred because they are available off-the-shelf, can be easily multiplexed, and are more suitable for burial. Curioni et al. (2018) found that for a range of fine-grained soils the current ASTM D6780/D6780M standard (ASTM 2012) did not produce accurate results when using multiplexers, usually necessary in field monitoring applications due to the number of probes required, and proposed to replace eq. (2) with a simplified equation that led to better precision and accuracy (eq. (3)). Further details on this procedure are described later in the section titled "Laboratory calibration", full details can be found in Curioni et al. (2018).

$$(3) \quad V_r \frac{\rho_w}{\rho_d} = a_2 + b_2 (V_1 \sqrt{K_a})^2$$

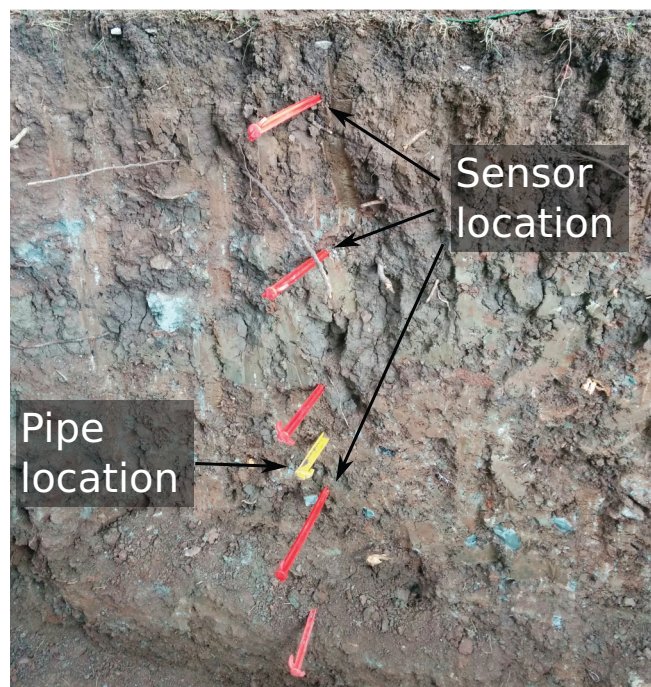
Measuring  $w$  and  $\rho_d$  continuously in the field offers the opportunity of monitoring changes of a wide range of soil properties with TDR, including, e.g.,  $S_r$ , porosity, void ratio, and air content. It is proposed that this method could be used as an assessment tool during long-term soil condition monitoring and incorporated in early-warning systems that trigger alarms based on approaching saturation levels or on significant and potentially problematic relative change. The method is simple, easily interpreted, and does not require specific assumptions to be made. Similarly to alternative sensing techniques that can be used for condition monitoring (e.g., piezometers, inclinometers), the main disadvantage of the proposed method is that it requires the installation of a potentially large number of sensors for mapping the spatial variation of the soil, depending on the desired spatial resolution. However, point sensors provide highly detailed information at point locations (the volume measured by TDR is typically of the order of  $0.001 \text{ m}^3$ ) and are well suited for monitoring changes with time. As TDR works on EM principles, it can be combined effectively with other shallow geophysical techniques, e.g., ERT or ground penetrating radar (GPR). The TDR measurements could be used for calibration purposes and allow for monitoring of larger volumes of soil.

## Field case study

### Site characterization

A grass-covered field test site surrounded by large conifer trees, approximately 10 m by 10 m, was developed at Blagdon in North Somerset (UK) in collaboration with Bristol Water plc. The site geology belongs to the Sidmouth Mudstone Formation of the Mercia Mudstone Group characterized by red-brown mudstone and siltstone (Fig. 2). The shallow soil belongs to the Whimble 3 soil association consisting of "reddish fine loamy or fine silty over clayey soils with slowly permeable subsoils and slight seasonal waterlogging" (National Soil Resources Institute 2015). In the same report, the ground movement potential for this soil was classified as moderate. Laboratory analyses of samples collected

Fig. 2. Investigated soil at Blagdon, UK, and approximate positions of sensors (red pegs) and pipe (yellow peg). [Color online.]



from the site confirmed these classifications and the main characterization parameters are reported in Table 1. The dominant clay minerals determined with X-ray diffraction (XRD) analysis were approximately two-third illite and one-third smectite clay and approximately 50% of minerals were found to be of the clay type.

Weathered Mercia Mudstone has some relatively unusual geotechnical properties. This material was formed in the Triassic period in "mainly arid, continental deposition" conditions (Hobbs et al. 2002) and included aeolian and alluvial deposition mechanisms. This has resulted in the nonhomogeneous distribution of clay content within the soil; indeed, it is common to encounter aggregations of clay particles: agglomerations of clay particles forming larger particle sizes (silt sized or larger if "weakly cemented" via precipitates; Hobbs et al. 2002). Whilst the clay minerals encountered on site are relatively active, the aggregation ratio (i.e., the ratio of clay content from mineralogical analysis to clay content from particle-size distribution, indicating the presence of aggregates) is known to be high in this material (Hobbs et al. 2002). This suggests that the influence of the clay content on the soil fabric was not as pronounced as could be expected from the classification of the soil. The aggregation ratio was estimated to be approximately 2 from XRD and particle-size distribution analysis indicating that the clay minerals of the studied soil were locked away in aggregates and explaining the seemingly unusual behavior seen in the field (e.g., the high hydraulic conductivity, as discussed later), despite the soil classification and the high plasticity measured. It should also be noted that a high variation was measured in the determination of the LL (separate tests resulted in values ranging from 57% and 67%) and that the median value of 65% was used to give a general indication of the soil behavior, but might not be fully representative of the conditions encountered in the field, particularly given the presence of clay aggregates.

### Field setup

Two trenches of dimensions 8 m × 1.2 m × 1.2 m (length × width × height) were excavated and the excavated soil was used to restate the trench to achieve similar conditions to the original ma-

**Table 1.** Characterization parameters of the soil studied.

| Parameter                             | Value                                    |
|---------------------------------------|--|
| Soil type (BSI 2015)                  | MH: clayey sandy silt of high plasticity |
| Gravel (%w)                           | 4  |
| Sand (%w)                             | 36                                       |
| SILT (%w)                             | 29                                       |
| Clay (%w)                             | 31                                       |
| Plastic limit (%)                     | 37                                       |
| Liquid limit (%)                      | 65                                       |
| Plasticity index (%)                  | 26                                       |
| Linear shrinkage (%)                  | 13                                       |
| Particle density (Mg/m <sup>3</sup> ) | 2.66                                     |

terial. With the exception of the data used for validation purposes (see section titled “Final sampling validation”), only the results obtained from one of these trenches are discussed. The second trench was investigated with noninvasive geophysical techniques (i.e., multi-channel analysis of surface waves (MASW) and ERT) and a limited number of TDR sensors, and the results are discussed elsewhere (unpublished manuscripts). The soil was compacted in layers approximately 0.1–0.2 m thick using a Kango trench compactor. During the backfilling process, a number of TDR and temperature sensors were buried at different depths relative to the pipe (Figs. 2 and 3b). These sensors were buried both at the centerline of the pipe (above and below the pipe) and also at lateral distances on both sides of the pipe, as shown in Fig. 3b. The pipe was specifically installed as part of the trial to generate controlled water leaks. In this paper, the leak was used as a mechanism to bring the soil to saturation levels (Fig. 3b) under controlled conditions. The pipe, buried at approximately 0.70 m from the surface, was sealed at one end and connected to a water network at the other end that was used to control the flow and pressure of the water entering the pipe. The point leak consisted of a 3 mm hole facing upwards. The hole was covered with geotextile to stop solid particles entering the pipe and to avoid pressurized water to be directly injected into the soil, as the purpose of the experiment was to saturate the soil from within and not to study the effect of pressurized pipe leakage on the soil. Sensors were installed at two locations: one next to the point leak and one approximately 5 m away to be used as a control and not directly affected by the saturation experiments (Fig. 3a).

The TDR sensors used in this study were three-rod CS635 probes, 150 mm long with a 6 m LMR200 low-loss cable (Campbell Scientific, Logan, USA). The probes were connected to a single TDR100 device using SDMX 50  $\Omega$  multiplexers and additional 0.5 m cables. The total cable length was kept to a minimum to minimize signal attenuation. The TDR waveforms collected in this study were saved and later analyzed to find  $K_a$  using the tangent method (Heimovaara 1993; Curioni et al. 2012). Temperature sensors (model 107, Campbell Scientific, Logan, USA) were also installed in the field corresponding to each TDR probe so that temperature correction could be applied to the measurements. In addition, three vibrating wire piezometers (model W4, Soil Instruments Ltd., Uckfield, UK) and five negative water pressure sensors (model MPS6, METER Group Inc., Pullman, WA, USA) were installed at different depths on one side of the pipe for monitoring the pore-water pressures in the soil. The monitoring station consisted of a CR6 datalogger and AM16/32B multiplexer positioned in a nearby cabinet. Power was provided by a combination of deep-cycling batteries and a solar panel. A WXT520 weather station (Vaisala, Helsinki, Finland) was also installed next to the cabinet.

## Laboratory calibration

The TDR probes were individually calibrated in the laboratory using the final setup deployed in the field and following procedures reported in the literature (Heimovaara 1993; Robinson et al. 2003a, 2003b; Curioni et al. 2012). The reference materials used for the calibration of the probes were air, acetone, and water. Bulk samples of subsoil collected during field installation were used to develop a soil-specific calibration following the method reported by Curioni et al. (2018). The method consists of taking TDR measurements while performing a standard compaction test and applying two fitting procedures between the parameters shown in Figs. 4b and 4c and using eqs. (1) and (3). Following the determination of the soil-specific coefficients, eqs. (1) and (3) (Table 2) can be rearranged to find  $w$  and  $\rho_d$ . As shown in Figs. 4b–4d, physical constraints were added to the relationships (i.e., for  $w$  (or  $\theta$ ) = 0%:  $\rho_d = 1 \text{ Mg/m}^3$ ,  $K_a = 1$ ,  $V_1 = 0$ ,  $V_r = 0$ ; for  $w$  (or  $\theta$ ) = 100%:  $\rho_d = 1 \text{ Mg/m}^3$ ,  $K_a = 81$ ). The constraints for  $V_1$ ,  $V_r$ , and  $K_a$  are based on their theoretical values in air and in pure water. The lower limit of  $1 \text{ Mg/m}^3$  assigned to  $\rho_d$  (i.e., corresponding to the density of water) was considered appropriate for this study, but caution should be used in specific situations. Certain soils, e.g., peat, highly rich in organic matter and highly porous, can have  $\rho_d$  values lower than  $1 \text{ Mg/m}^3$ . The same can occur in other highly porous materials. However, shallow mineral soils are typically expected to exhibit densities higher than  $1 \text{ Mg/m}^3$  and this is the case for UK shallow soils, including the soil studied in this paper (confirmed during discussions with the British Geological Survey and while searching their records). Figure 4a shows the compaction curve for the soil studied. For a detailed analysis of the laboratory procedure, the reader is referred to Curioni et al. (2018). Using the same dataset, an independent soil-specific calibration was developed by fitting a third-order polynomial similar to Topp et al. (1980) (Fig. 4d; Table 2). As seen in Fig. 4d, the difference between the soil-specific polynomial and the Topp et al. (1980) equation was relatively small for the soil studied, with deviations of  $\theta$  typically smaller than 3%.

In this study, a temperature correction was applied to  $K_a$ ,  $V_1$ , and  $V_f$  using the empirical equations suggested by Jung et al. (2013b) for fine-grained soils (eqs. (4)–(7)).

$$(4) \quad K_{a \text{ cor}} = (1.02 - 0.0010T)K_a$$

$$(5) \quad V_{1 \text{ cor}} = (1.06 - 0.0030T)V_1$$

$$(6) \quad V_{f \text{ cor}} = \left[ \frac{2}{\frac{V_f}{V_i}(1 - \text{TCF}_\sigma) + 2\text{TCF}_\sigma} \right] V_f$$

$$(7) \quad \text{TCF}_\sigma = 2.04 - 0.347 \ln(T)$$

where  $K_{a \text{ cor}}$ ,  $V_{1 \text{ cor}}$ , and  $V_{f \text{ cor}}$  are the corrected parameters corresponding to a reference temperature (in this study, 20 °C);  $T$  is the temperature at the time of the measurement (°C);  $V_i$  is the input voltage as shown in Fig. 1; and  $\text{TCF}_\sigma$  is the temperature correction factor for bulk electrical conductivity (Jung et al. 2013b).

## Monitoring program

The soil field monitoring started in November 2015 and lasted approximately 20 months. Measurements were taken from the buried sensors at 4 h intervals, except during saturation tests when the rate of sampling was increased to every hour. The ground was saturated during three controlled saturation experiments conducted in 2016 during different seasons. Further details of the experiments are shown in Table 3. The site was manually dug at the end of the monitoring period in June 2017 and undisturbed soil samples were taken using cylinders of volume between 400 and 500 cm<sup>3</sup> in proximity of selected TDR probes for

Fig. 3. Details of field test site: (a) plan view and (b) cross section showing instrumentation layout. [Color online.]

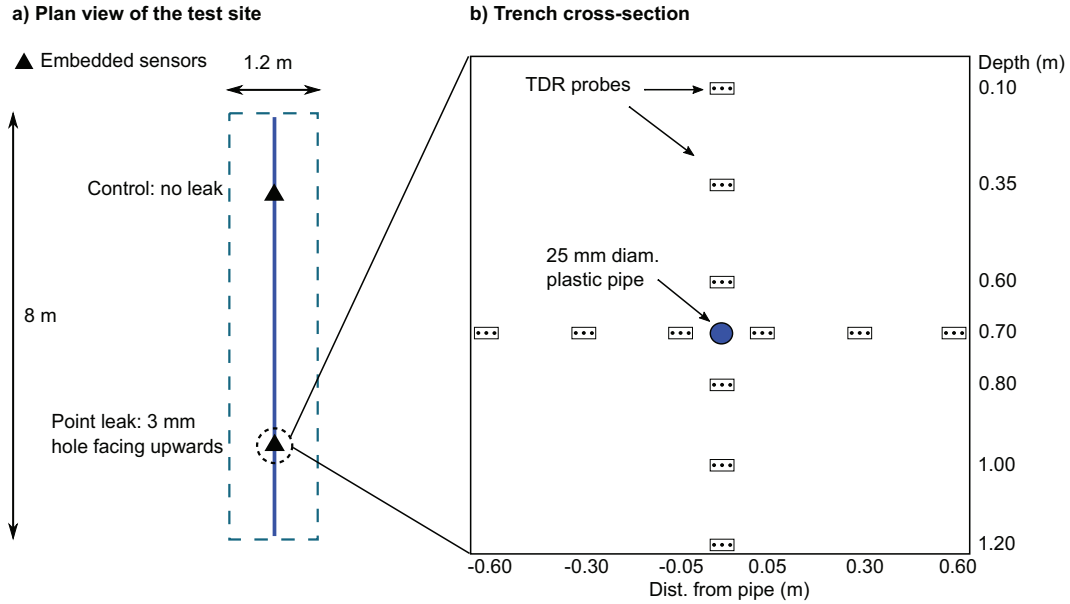


Fig. 4. Soil-specific laboratory calibration: (a) compaction curve; (b) step 1 of moisture–density soil-specific calibration; (c) step 2 of moisture–density soil-specific calibration; (d) soil-specific and Topp et al. (1980) polynomials.

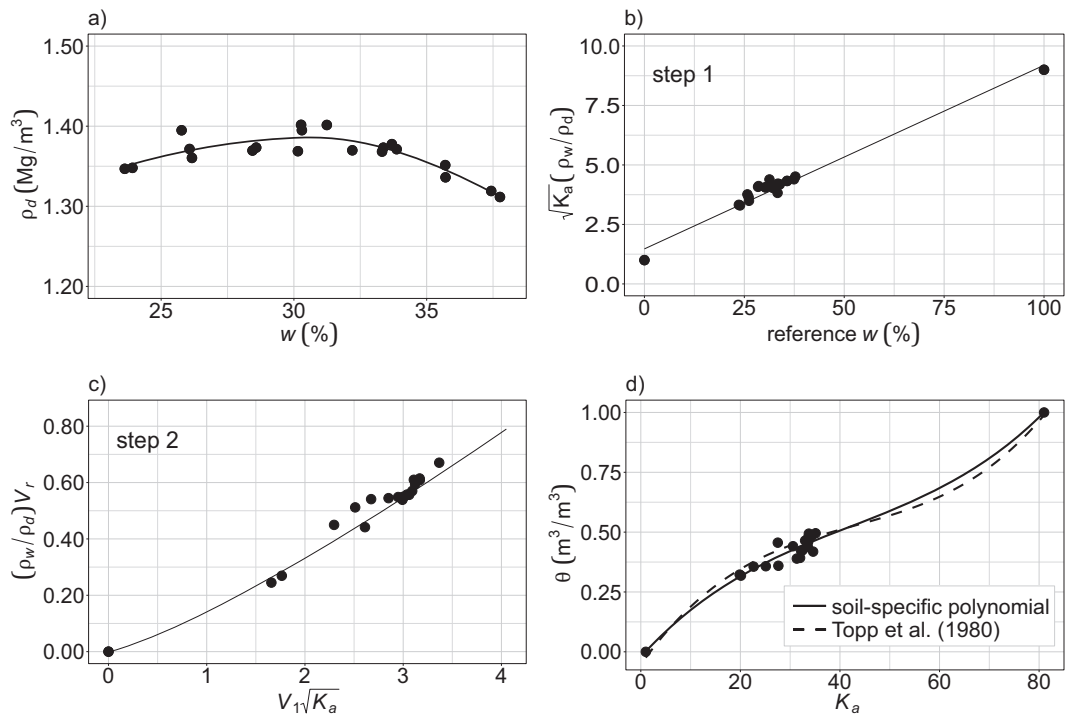


Table 2. Soil-specific and Topp et al. (1980) calibration coefficients.

|   | $a_1$                 | $b_1$                 | $a_2$                  | $b_2$                 | $c_2$  |
|---|-----------------------|-----------------------|------------------------|-----------------------|--------|
| Soil-specific moisture–density calibration (eqs. (1) and (3)) | 1.5692                | 0.0767                | 0                      | 0.1487                | 1.2005 |
| $y = a + bx + cx^2 + dx^3$                                    | $a$                   | $b$                   | $c$                    | $d$                   |        |
| Soil-specific polynomial                                      | $-7.6 \times 10^{-2}$ | $2.75 \times 10^{-2}$ | $-4.78 \times 10^{-4}$ | $3.77 \times 10^{-6}$ |        |
| Topp et al. (1980)  | $-5.3 \times 10^{-2}$ | $2.92 \times 10^{-2}$ | $-5.5 \times 10^{-4}$  | $4.3 \times 10^{-6}$  |        |

Table 3. Details of the controlled saturation experiments conducted in this study.

| Saturation test         | Duration (h) | Volume of water (m <sup>3</sup> ) | Mean flow rate (L/min) | Pressure (bar) |
|-------------------------|--------------|-----------------------------------|------------------------|----------------|
| Leak1_Apr (2016)        | 25.75        | 5.20                              | 3.366                  | 1.5            |
| Leak2_Jul (2016)        | 162.33       | 26.22                             | 2.962                  | 4              |
| Leak3_Dec (2016)        | 121.50       | 18.69                             | 2.564                  | 4              |
| Validation March (2018) | 18.00        | 5.78                              | 5.402                  | 4              |

Note: 1 bar = 100 kPa.

Can. Geotech. J. Downloaded from www.nrcresearchpress.com by 192.171.188.42 on 08/22/19  
For personal use only.

validation purposes. Additional undisturbed samples next to the TDR probes were taken in March 2018 after running another saturation experiment (Table 3) for validation during extreme wetting conditions. It was decided to not excavate the soil for intrusive sampling during the monitoring period to avoid disturbing the equipment setup and to avoid changing the soil conditions artificially; hence, compromising the test. Additional pore-water pressure sensors were included (positive and negative), although unfortunately the negative water potential probes failed to return useful data.

## Results and discussion

### Long-term soil monitoring

Figure 5 shows the daily variation of soil parameters with depth measured by TDR and temperature sensors during the entire monitoring period for both measurement locations (i.e., control and point leak, see Fig. 3). Daily rainfall data are also presented in Fig. 5. Using eqs. (1) and (3), the TDR parameters extracted during waveform analysis were converted to soil  $\rho_d$  and  $w$ . The TDR readings showed an initial step change after a few weeks from installation, following the first significant rainfall events occurring in early January 2016. This change indicates soil particle rearrangement and the establishment of good contact between the soil and TDR probes. It is known that the presence of large air gaps next to the rods relative to the rod diameter and spacing can affect the reliability of the results (Ferré et al. 1996; Knight et al. 1997) and the establishment of a good contact is important to collect high-quality data. In shrink-swell soils, the contact can be lost during drying events. However, due to the absence of prolonged dry periods, coupled with the behavior of the clay in this soil, this was not considered a problem in this study. Due to the calibration being conducted on subsoil samples, the measurements were expected to be less reliable in the topsoil (i.e., <0.2 m) and this is shown by the more erratic behavior of the probes buried at 0.10 m. The three spikes in the measured  $w$  at the point leak location correspond to the three saturation experiments conducted in 2016. The site was covered by a large tree canopy and therefore the site was not expected to change drastically during single rainfall events, and it is clear that the natural variation of the soil conditions caused by rainfall was significantly smaller compared to the variation induced by the leaks. The three saturation experiments were of different sizes (see Table 3); however, even the smaller one (i.e., leak1\_Apr) induced significant changes in the surrounding soil. The presence of a large tree canopy limited the site exposure to direct sunlight and the absence of a prolonged dry period during the monitoring time is believed to be the reason why  $w$  did not reduce drastically during the summer of 2016. This is not unusual in the UK and past climatic records from nearby weather stations (e.g., Yeovilton, Met Office 2018) confirm that on average, daily air temperatures are rarely higher than 20 °C during the summer and rainfall is relatively evenly distributed throughout the year.

Two important considerations for the TDR method used in this study can be discerned from Fig. 5. As a result of the soil-specific calibration, the TDR probes at the control location (i.e., not influenced by the saturation experiments) measured a slight increase in  $\rho_d$  over time. Although an independent assessment of the rising values of  $\rho_d$  was not carried out, this result is promising because the trench backfill would be expected to settle naturally with time and demonstrates the high sensitivity of the TDR technique. TDR measurements are not expected to drift over time, and considering that the trend was measured by multiple probes it seems plausible that this is an indication of soil settlement and densification over time. Final validation (see section titled “Final sampling validation”) showed relatively good agreement between the  $\rho_d$  measured physically by intrusive sampling and by TDR under unsaturated conditions.

In addition, following temperature correction (Jung et al. 2013b), the method was insensitive to the temperature variations experienced on site. This is an important result because TDR is an EM technique and the EM parameters are known to depend on temperature, particularly electrical conductivity (Rinaldi and Cuestas 2002; Persson and Berndtsson 1998; Yu and Drnevich 2004; Jung et al. 2013b).

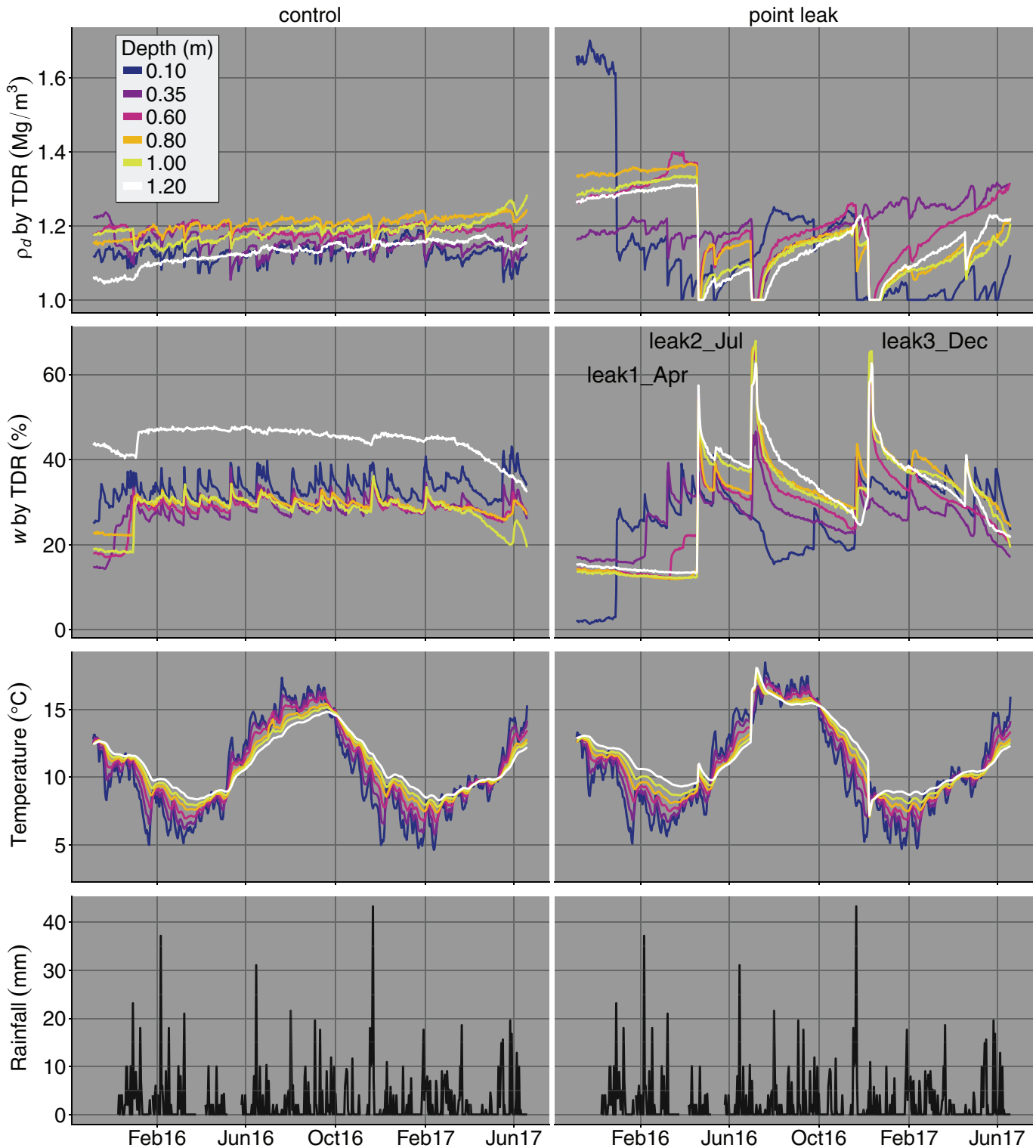
Figure 5 confirms the ability of TDR to measure both trends and abrupt changes over time. The rapid decrease in  $\rho_d$  shown in Fig. 5 during the saturation experiments is believed to be unrealistic as the soil was not expected to exhibit large swelling over such a short time and only indicates that the ground went through a rapid and important change. However, following the saturation experiments the soil returned to equilibrium and the TDR derived  $\rho_d$  at both the control and leak locations became more similar (Fig. 5). It is worth mentioning that the TDR method for measuring  $\rho_d$  used in this paper has been shown to be accurate to within 5% from laboratory tests (Curioni et al. 2018) and, as it will be discussed later, to within 10% from field tests under unsaturated conditions (this study). This translates to an expected error of up to approximately 0.1–0.15 Mg/m<sup>3</sup>. Therefore, the differences measured between the control and point leak locations are typically within this range.

### TDR response at saturation

The results of the three saturation experiments conducted during different seasons in 2016 are shown in Fig. 6. For simplicity, only the results from the vertical array of probes located close-by the point leak are shown. The absence of spikes in  $w$  corresponding to the probes installed at the control location (Fig. 5) demonstrates that the injected water did not reach this location by flowing along the pipe or the trench, which in itself is an interesting result as this would be a natural flow path due to the disturbed nature of the soil compared to the unaffected soil outside the trench (this finding was independently confirmed with ERT surveys on a separate trench). The first saturation test was smaller compared to the others, as shown in Table 3. No attempts were made to remove occasional outliers; however, as some of the TDR probes recorded values of  $\rho_d$  below 1 Mg/m<sup>3</sup>, a lower boundary of 1 Mg/m<sup>3</sup> was applied to the data because shallow mineral soils, certainly in the UK, are expected to have densities greater than 1 Mg/m<sup>3</sup>. As explained earlier, this might not be the case in other soils and conditions and constraining density may not always be appropriate. The fact that some values went below this threshold is an indication that the TDR measurements at saturation were not particularly accurate. This is probably due to the different domain used to develop the soil-specific calibration, which did not cover the near-saturation range (due to the impracticality of conducting a standard compaction test at near-saturation conditions) and it indicates that eqs. (1) and (3) may not cope well at extreme wetting conditions. However, a sudden large change in both  $\rho_d$  and  $w$  was measured by the TDR sensors as soon as the saturation tests were started (note that the rate of sampling was increased to one full set of measurements from all the probes per hour), confirming that TDR was able to detect the rapid and abrupt change occurring in the system. It is worth stressing that the ability to detect significant changes is of utmost importance for applications such as asset health monitoring.

The sudden ingress of water caused the soil immediately surrounding the pipe to approach saturation and experience small localized expansion for the duration of the tests, allowing the water to fill the pores and causing  $\rho_d$  to decrease slightly. The slight decrease of  $\rho_d$  was confirmed with intrusive sampling conducted immediately after stopping a saturation test (see section titled “Final sampling validation”). Due to the presence of geotextile on the pipe, the water in the soil was not expected to reach high positive pressures. This was independently confirmed by the measurements of positive pore-water pressure sensors located

Fig. 5. Daily variation of  $w$ ,  $\rho_d$ , and temperature with depth (note that leaking pipe was buried at 0.70 m depth), and daily rainfall measured during entire monitoring period and for both measurement locations. [Color online.]



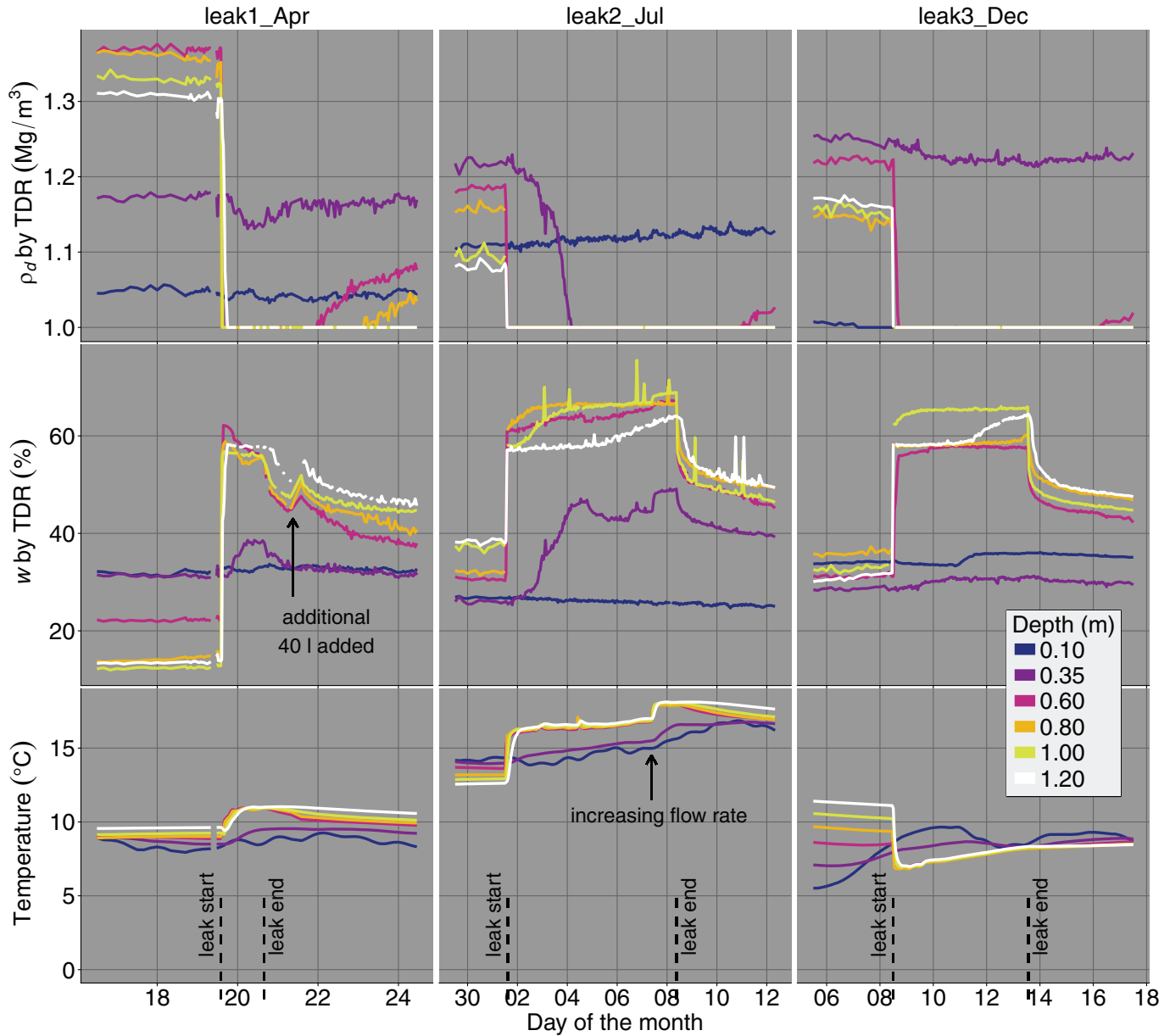
near the leak, which measured negligible positive pressures smaller than 2 kPa during the saturation experiments. In addition, final validation sampling brought no evidence of voids around the leak.

Following the saturation experiments, the values of  $\rho_d$  remained lower than before (also compared to the control point, see Fig. 5) and increased slowly over time in a matter of weeks. This

increase might indicate particle rearrangement and densification following softening caused by the saturation experiments. However, from the measured data and considering the aggregation ratio of the clay, coupled with the large volume of water exiting the pipe, it is suggested that the soil on site was behaving more akin to a cohesionless soil than a fine-grained, high-plasticity, low hydraulic conductivity material that the classification might sug-

Can. Geotech. J. Downloaded from www.nrcresearchpress.com by 192.171.188.42 on 08/22/19  
For personal use only.

Fig. 6. Variation of  $w$ ,  $\rho_d$ , and temperature with depth during controlled saturation experiments. [Color online.]

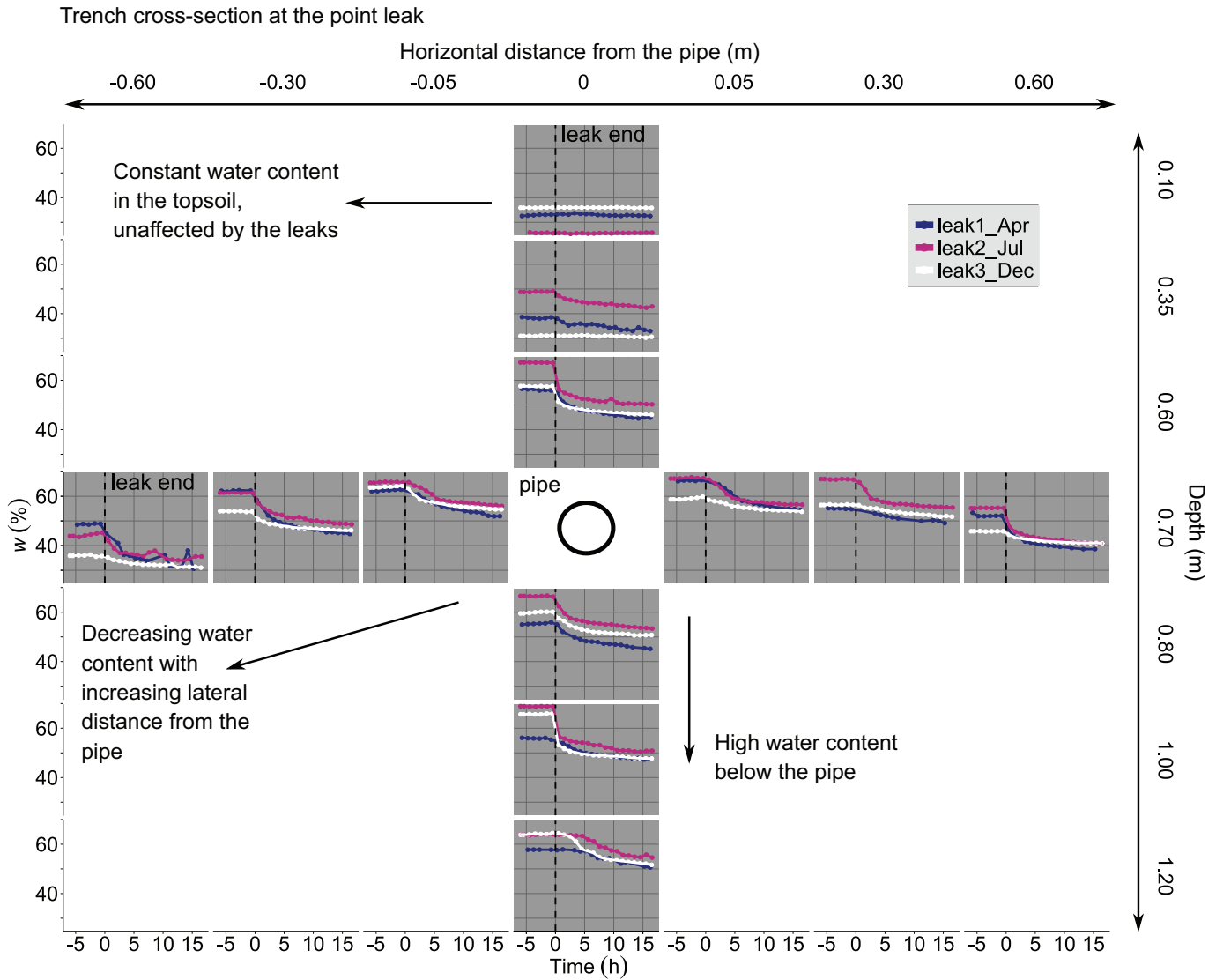


gest. The values of  $w$  during the saturation tests reached, and then stabilized, peak values, indicating that the soil reached a steady-state equilibrium at saturation (note that the data collection was briefly stopped a few hours after the end of the first saturation test and an additional 40 L of water was introduced into the soil as part of a separate experiment not discussed here). As mentioned above, the soil-specific calibration (eqs. (1) and (3)) was developed on samples at a lower range of water contents and therefore the absolute values of  $w$  measured by TDR at near saturation were less reliable (see section titled “Final sampling validation”). However, it is important to stress that the absolute values are less important for the detection of extreme conditions (e.g., when approaching saturation) and that it is sufficient to detect significant changes compared to prior conditions (or compared to an expected range of values) to indicate potential problems. TDR was clearly able to detect the sudden significant changes induced by an extreme event (in this case the ingress of water from a leaking pipe), and this result validates the proposed approach of using TDR for monitoring geotechnical assets.

Figure 6 also shows the change in soil temperature during these experiments. The magnitude of change varied and was between approximately 2 and 6 °C. The change was due to the temperature difference between the water in the pipe and the soil. In April and July the temperature of the water was higher and caused the soil temperature to increase; in December the opposite was observed. It was also found that the temperature was sensitive to changes in flow rate. During the second saturation experiment (i.e., leak2\_Jul), a second step change in temperature was recorded when the flow rate was manually increased towards the end of the experiment. Despite these changes, the measurements of  $w$  and  $\rho_d$  by TDR remained largely insensitive to the temperature variation.

The measurements of  $w$  from all the TDR probes installed in a star configuration around the pipe at the point leak location (see Fig. 3) corresponding to the end of the three saturation experiments are shown in Fig. 7. The measurements demonstrate the TDR ability to provide both spatial and temporal information on the soil conditions. During the different saturation experiments the water followed different flow paths and went predominately

Fig. 7. Spatial and temporal variation of  $w$  around pipe at point leak location (see Fig. 3) corresponding to end of three saturation experiments. [Color online.]



downwards and to a slightly lesser extent to the sides without reaching the surface. This is evidenced by the smaller magnitude of  $w$  with increasing lateral distance from the pipe, suggesting that the largest changes were restricted to the region immediately close to the pipe. None of the 12 probes installed in a star configuration around the pipe at the control location measured an increase in  $w$  for the duration of the saturation experiments, confirming that the water did not flow preferentially along the trench. Figure 7 also shows that the water content levels reached at the end of each experiment were not constant (i.e., values at negative times in Fig. 7 before the leak was closed) and that the dissipation of water after stopping the leaks was dependent upon these levels. Typically, a sharp drop in  $w$  and subsequent levelling of the values was measured within the first 5 h after stopping the inflow of water. Subsequently, pre-leak levels were reached several days later (see Fig. 5). The nature of the soil studied potentially explains the comparatively high draining behavior immediately after stopping the water ingress. As described earlier in the section titled “Site characterization”, the soil originated from weathered Mercia Mudstone and consisted of a mix of clay minerals in similar proportions with particles of sand and silt size. Direct analysis (XRD and particle-size distribution) and previous studies

(Hobbs et al. 2002) suggest that the clay minerals formed larger aggregates and therefore the soil did not behave as might be expected from the high plasticity of the soil.

**Final sampling validation**

At the end of the monitoring period (approximately 20 months) undisturbed soil samples were taken using cylinders of known volume to validate the TDR measurements (note that the results from the second trench, trench2, are also reported here; see previous section titled “Field setup”). Additional validation samples were also taken 9 months later at the point leak location on trench1 at or close to saturation. Tables 4 and 5 show the comparison between the reference  $w$  and  $\rho_d$  obtained by direct measurement of the sample volumes and masses and the values measured by TDR. Note that because the excavations were conducted manually to minimize disruption, the samples were only taken at or in the proximity of a selection of the TDR probes. Table 4 demonstrates the relatively good accuracy achieved by TDR under unsaturated conditions, with mean absolute errors of approximately 2.5% and 0.09 Mg/m<sup>3</sup> ( $\approx 7\%$ ) for  $w$  and  $\rho_d$ , respectively. These mean errors were calculated including the samples taken in the topsoil, which showed higher errors up to approximately 7% for  $w$  and 17%

Can. Geotech. J. Downloaded from www.nrcresearchpress.com by 192.171.188.42 on 08/22/19 For personal use only.

**Table 4.** Validation of the TDR measurements at the end of the monitoring period (June 2017) under unsaturated conditions.

| Position                   | Depth (m) | $\rho_d$ by TDR (Mg/m <sup>3</sup> ) | w by TDR (%) | Reference $\rho_d$ (Mg/m <sup>3</sup> ) | Reference w (%) | Error $\rho_d$ (Mg/m <sup>3</sup> )* | or w (%)*          |
|----------------------------|-----------|--------------------------------------|--------------|---|-----------------|--------------------------------------|--------------------|
| Control (topsoil)          | 0.10      | 1.12                                 | 33.93        | 1.36                                    | 26.11           | -0.24 [17.6]                         | 7.82 [30.0]        |
| Control (subsoil)          | 0.35      | 1.18                                 | 25.27        | 1.40                                    | 21.85           | -0.22 [15.7]                         | 3.42 [15.7]        |
|                            | 0.60      | 1.21                                 | 26.52        | 1.34                                    | 23.26           | -0.13 [9.7]                          | 3.26 [14.0]        |
|                            | 0.70      | 1.23                                 | 24.70        | 1.31                                    | 22.07           | -0.08 [6.1]                          | 2.63 [11.9]        |
| Point leak (topsoil)       | 0.10      | 1.12                                 | 23.00        | 1.18                                    | 22.52           | -0.06 [5.1]                          | 0.48 [2.1]         |
| Point leak (subsoil)       | 0.35      | 1.31                                 | 17.07        | 1.27                                    | 17.63           | 0.04 [3.1]                           | -0.56 [3.2]        |
|                            | 0.60      | 1.32                                 | 19.75        | 1.31                                    | 22.52           | 0.01 [0.8]                           | -2.77 [12.3]       |
|                            | 0.70      | 1.20                                 | 25.92        | 1.23                                    | 21.87           | -0.03 [2.4]                          | 4.05 [18.5]        |
| Trench2                    | 0.35      | 1.19                                 | 29.11        | 1.10                                    | 30.06           | 0.09 [8.2]                           | -0.95 [3.2]        |
|                            | 0.60      | 1.23                                 | 29.03        | 1.12                                    | 30.26           | 0.11 [9.8]                           | -1.23 [4.1]        |
|                            | 0.80      | 1.23                                 | 27.55        | 1.22                                    | 27.80           | 0.01 [0.8]                           | -0.25 [0.9]        |
| <b>Mean absolute error</b> |           |                                      |              |   |                 | <b>0.09 [7.2]</b>                    | <b>2.49 [10.5]</b> |

\*Values in square brackets are % error.

**Table 5.** Additional validation of the TDR measurements (March 2018) at partially saturated and saturated conditions; position is "point leak" in all cases presented.

| Saturation                 | Depth (m) | $\rho_d$ by TDR (Mg/m <sup>3</sup> ) | w by TDR (%) | Reference $\rho_d$ (Mg/m <sup>3</sup> ) | Reference w (%) | Error $\rho_d$ (Mg/m <sup>3</sup> )* | Error w (%)*        |
|----------------------------|-----------|--------------------------------------|--------------|---|-----------------|--------------------------------------|---------------------|
| Partially saturated        | 0.70      | 1.00                                 | 55.47        | 1.31                                    | 37.05           | -0.31 [23.7]                         | 18.42 [49.7]        |
|                            |           | 1.12                                 | 24.67        | 1.19                                    | 40.37           | -0.07 [5.9]                          | -15.70 [38.9]       |
|                            |           | 1.00                                 | 56.96        | 1.26                                    | 46.45           | -0.26 [20.6]                         | 10.51 [22.6]        |
|                            |           |                                      | 58.33        | 1.33                                    | 35.49           | -0.33 [24.8]                         | 22.84 [64.4]        |
|                            |           |                                      | 52.51        | 1.28                                    | 38.71           | -0.28 [21.9]                         | 13.80 [35.6]        |
| Saturated                  | 0.70      | 1.00                                 | 57.87        | 1.26                                    | 46.45           | -0.26 [20.6]                         | 11.42 [24.6]        |
|                            |           |                                      | 58.11        | 1.31                                    | 37.05           | -0.31 [23.7]                         | 21.06 [56.8]        |
|                            |           |                                      | 56.13        | 1.02                                    | 50.73           | -0.02 [2.0]                          | 5.40 [10.6]         |
|                            |           |                                      | 59.62        | 1.13                                    | 45.81           | -0.13 [11.5]                         | 13.81 [30.1]        |
|                            |           |                                      | 67.86        | 1.12                                    | 52.04           | -0.12 [10.7]                         | 15.82 [30.4]        |
|                            |           |                                      | 58.96        | 1.21                                    | 45.13           | -0.21 [17.4]                         | 13.83 [30.6]        |
| <b>Mean absolute error</b> |           |                                      |              |   |                 | <b>0.21 [16.6]</b>                   | <b>14.78 [35.9]</b> |

\*Values in square brackets are % error.

for  $\rho_d$ , but this was expected given that the soil-specific calibration was conducted on subsoil samples only. For completeness, Table 4 also shows the percentage error for both  $w$  and  $\rho_d$ . These values can be useful for comparison exercises, but can be misleading. The absolute errors are more meaningful because they give a direct idea of the expected accuracy in the measurements. For example, a percentage error for  $w$  of over 10% seems unsatisfactory, but the corresponding absolute values are within approximately 3% water content, which is often within the accuracy range of soil moisture sensors.

These results are very promising because they demonstrate that the TDR sensors remained relatively accurate after a significant period of time and even after the soil had been subjected to important changes, in this case three wetting cycles. This is important and it indicates that TDR sensors can be relied upon even after the soil reaches saturation and therefore, potentially, after applying mitigation measures.

However, during severe wetting the absolute values measured by TDR were less reliable. A number of samples were taken following a final saturation test (for details see Table 3), some taken immediately after stopping the leak ("saturated" in Table 5) and some taken in close proximity 6 h later ("partially saturated" in Table 5). Some of the variation shown is due to soil heterogeneity and to preferential water movement; however, it is evident that TDR generally underestimated  $\rho_d$  and considerably overestimated  $w$ , with average errors of 0.21 Mg/m<sup>3</sup> for  $\rho_d$  and, remarkably, of over 10% for  $w$  (with some errors greater than 20%). It is impossible to know if these errors were similar during the saturation tests conducted prior to the first disturbance caused by the first intrusive sampling. However, given the very large  $w$  (sometimes greater than LL) measured by TDR during the previous saturation experiments, and given that some probes measured a sharp and un-

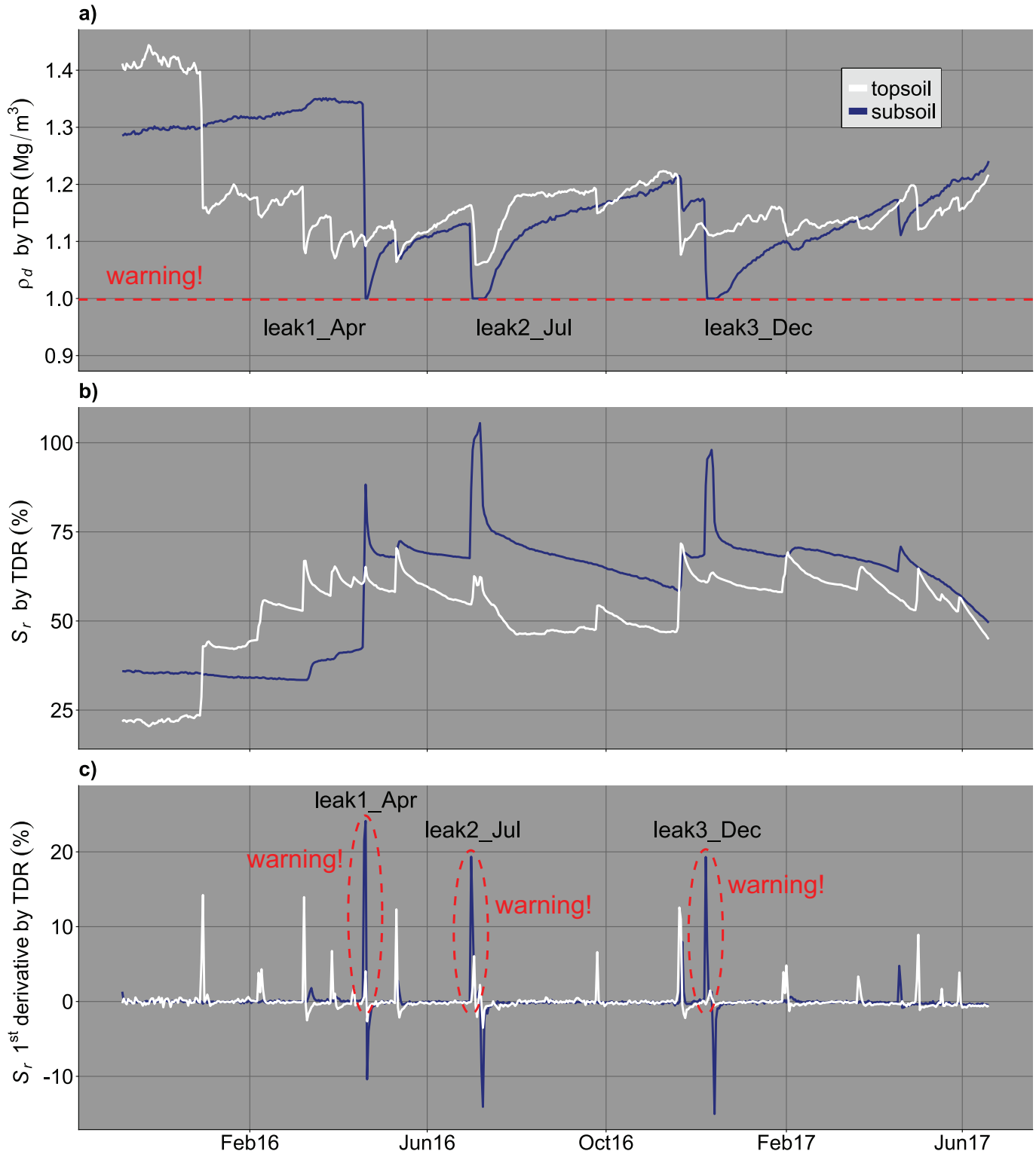
realistic drop in  $\rho_d$  (Figs. 5 and 6), it is probable that the TDR measurements were also less accurate in these cases. As mentioned above, this is likely due to the fact that the calibration was conducted at lower water contents and perhaps eqs. (1) and (3) simply could not cope at extreme wetting conditions following the sudden changes induced by the leaks. However, these important changes were more clearly highlighted due to the magnified measurements by TDR and can effectively be exploited for relative health monitoring of geotechnical assets.

#### Early warnings from TDR

Results presented in the previous sections demonstrate the ability of TDR to measure both  $w$  and  $\rho_d$  over a relatively long time period with relatively good accuracy under unsaturated conditions. These two soil parameters provide the opportunity of calculating a wide range of soil properties using a single technique, including, e.g., the  $S_r$ , porosity, and air content (BSI 1999b). These properties are linked to the strength of the soil (particularly the soil saturation level) and provide an indication of the soil stability. In the case of geotechnical assets, such as earth dams, embankments, cuttings, levees, and slopes, it is proposed that TDR be included as part of a monitoring system that sends early warnings based on specific thresholds of the measured soil parameters. Depending on the soil values with respect to pre-defined thresholds (absolute and (or) based on relative change), the system could be used to prompt inspections or interventions. Considering the results from this study and the suboptimal accuracy achieved by TDR under extreme wetting conditions, it is recommended that the system should not rely solely on absolute values.

Although TDR can be used for quantitative monitoring if the soil in the field is within the range tested during calibration, the absolute values are less important when approaching extreme

**Fig. 8.** Soil (a)  $\rho_d$  and (b)  $S_r$  measured by TDR probes averaged according to oil layer in which they were installed (i.e., topsoil and subsoil), and (c) relative change of  $S_r$  expressed by its first derivative. Examples of warnings are shown based on the values of  $\rho_d$  and the large and abrupt relative change of  $S_r$ . [Color online.]

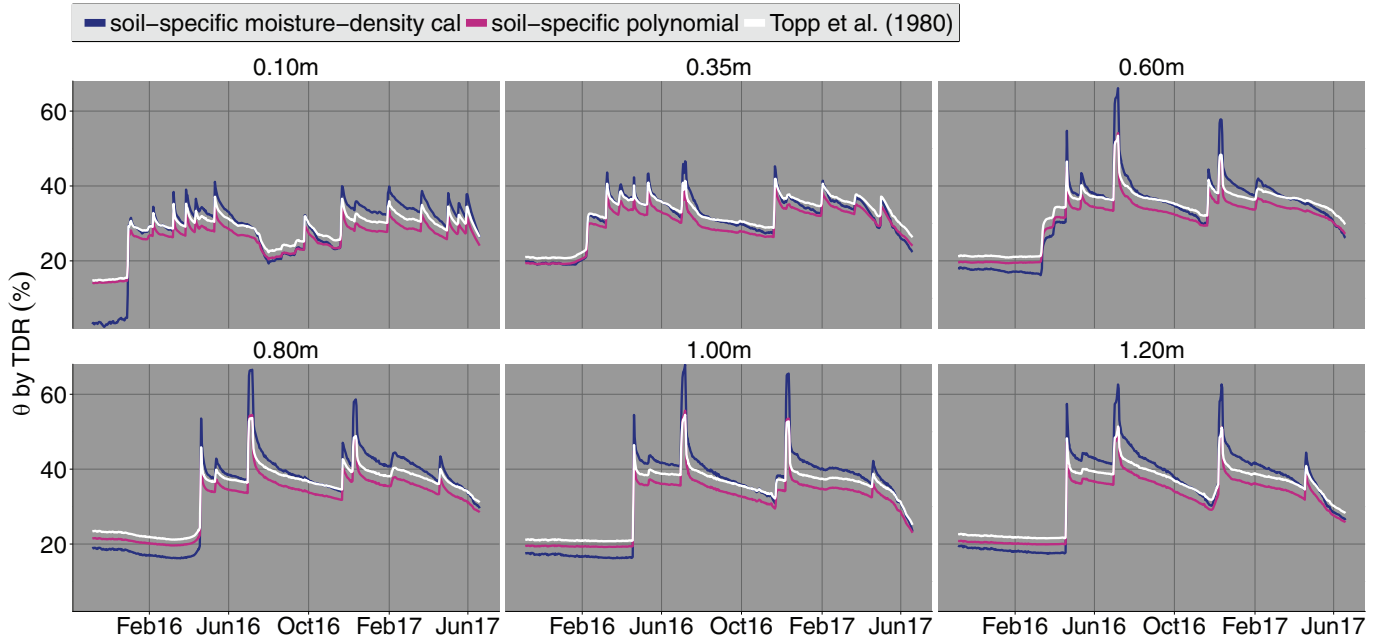


conditions. In order for a flag system approach to work, it would be sufficient for it to detect changes with respect to previous conditions or an expected range of values. The choice of thresholds for the warnings and interventions are user-defined and need careful consideration depending on the project. Practically, these thresholds and their interpretation would have to be defined by

an expert on a case-by-case basis and should account for the effective management of false alarms (e.g., manage the risks and costs associated with temporary service interruption of the asset). For the soil studied, absolute thresholds indicating potential problems could, e.g., be set based on  $\rho_d$  being equal (or lower, in case a threshold is not applied) to  $1 \text{ Mg/m}^3$ . As mentioned before, the soil

Can. Geotech. J. Downloaded from www.nrcresearchpress.com by 192.171.188.42 on 08/22/19  
For personal use only.

Fig. 9. Daily variation of  $\theta$  with depth calculated with different models for TDR probes located at point leak location. [Color online.]



was not expected to have densities lower than  $1 \text{ Mg/m}^3$  (this was confirmed during validation tests). During the saturation experiments, TDR measured values  $\leq 1 \text{ Mg/m}^3$  clearly indicating unusual and potentially problematic soil conditions. Due to the large TDR errors under extreme wetting conditions (see Table 5), it would be unwise to set warning thresholds based on the absolute values of  $w$  or on other parameters calculated using  $\rho_d$  and  $w$ , e.g.,  $S_r$ . However, large relative change can still be used to indicate potential problems. Figure 8 shows an example of warnings set based on the lower and unrealistic  $\rho_d$  values measured by TDR close to saturation (Fig. 8a) and based on the large and sudden change of  $S_r$  (expressed by its first derivative, Fig. 8c), which can be identified visually by applying a specific threshold or by using change detection algorithms (e.g., Sadeghioon et al. 2018; change detection algorithms are not discussed here as they are out of the scope of this paper). The absolute values of  $S_r$  (Fig. 8b) should not be trusted when approaching large values; however, they can still facilitate interpretation by an expert, e.g., in the decision of what constitutes a problematic change. Note that for simplicity and to reduce uncertainty, the measurements from multiple TDR probes were combined in Fig. 8 depending on the soil layer in which they were installed (i.e., topsoil and subsoil).

Traditionally, TDR has been used to measure  $\theta$  instead of  $w$ .  $\theta$  could also be used to provide early warnings but, if thresholds are based on absolute values, this requires knowledge of the saturated  $\theta$  to indicate approaching saturation conditions. However, the soil saturated  $\theta$  is not easily defined or measured, particularly in expansive soils and, for the soil studied,  $\theta$  would suffer from the same doubtful accuracy at extreme wetting conditions. The advantage of using  $w$  and  $\rho_d$  instead of  $\theta$  is that warning thresholds can be defined on multiple parameters and that, under unsaturated conditions, these parameters provide a more complete picture of the soil conditions, e.g., by estimating  $S_r$ , porosity, and air content. Figure 9 shows the values of  $\theta$  measured for the probes at the point leak location at different depths. The values were calculated using different calibration equations, i.e., Topp et al. (1980) polynomial, third-order soil-specific polynomial and soil-specific moisture–density calibration (Table 2). The three different models measured very similar trends although the absolute values typically varied by up to approximately 5%. These results indicate that the Topp et al. (1980) model provided comparable estimations of  $\theta$

to the soil-specific polynomial developed for the soil studied. Notably, the soil-specific calibration using eqs. (1) and (3) produced higher peak values during the saturation tests due to an underestimation of  $\rho_d$ . The use of separate models would provide better confidence in the measurements and would further support the interpretation of potentially problematic conditions by an expert.

To fully exploit the potential of using TDR for soil condition monitoring, it is suggested to combine the TDR technique with other shallow geophysical techniques. An obvious choice is ERT, which is suitable for permanent installations and can be used to map water movement over much larger volumes of soil typically of the order of tens or hundreds of cubic metres (Chambers et al. 2014; Gunn et al. 2015) compared to TDR probes that measure a volume of approximately  $0.001 \text{ m}^3$ , depending on the dimension of the probe (Robinson et al. 2003). The TDR measurements at point locations could be used to calibrate or facilitate the interpretation of ERT results. TDR could also be used to inform other shallow geophysical techniques such as GPR and MASW.

## Conclusions

Monitoring changes in ground properties is important in the analysis of stability of geotechnical assets and to monitor long-term deterioration processes. This study presented a novel application based on TDR technology for long-term monitoring of geotechnical assets, by monitoring relative change in soil gravimetric water content and density, key parameters that affect ground stability and its ability to support infrastructure. TDR sensors were buried in a clayey sandy silt that was exposed to water leaking from a pipe during controlled saturation experiments and the changes in the soil properties were measured under saturated and unsaturated conditions. Following soil-specific calibration, TDR sensors were able to provide detailed information on the temporal trends, but also on the magnitude of changes in the soil under unsaturated conditions with relatively good accuracy (i.e., typical errors  $<3\%$  for gravimetric water content and  $<10\%$  for dry density) after a 20 month period during which the soil had been subjected to significant changes. It was found that the accuracy decreased significantly during extreme wetting conditions. However, TDR was still clearly capable of detecting temporal changes.

It is proposed that TDR can be used for long-term condition monitoring of critical geotechnical assets (e.g., earth dams, embankments, levees) and for providing early warnings based on thresholds of parameters measured directly by TDR or on the detection of significant or unexpected change in the measurements. The proposed system would allow asset owners the opportunity to take action prior to failure of the asset by prompting inspections or interventions.

TDR could be used alone or in combination with other shallow geophysical techniques (e.g., ERT, MASW, GPR) so that larger volumes of soil could be mapped and monitored. Such an approach could be a real benefit to asset managers.

## Acknowledgements

The authors wish to thank the UK Engineering and Physical Sciences Research Council (EPSRC) for funding the research that underpinned this study via EPSRC Grant EP/KP021699/1. Special thanks go to Bristol Water plc for granting permission to conduct the field testing described in this study at one of their sites. This paper is published with the permission of the Executive Director of the British Geological Survey (NERC).

## References

- ASTM. 2003. Standard test method for water content and density of soil in place by Time Domain Reflectometry (TDR). ASTM standard D6780. ASTM, West Conshohocken, Pa.
- ASTM. 2005. Standard test method for water content and density of soil in place by Time Domain Reflectometry (TDR). ASTM standard D6780. ASTM, West Conshohocken, Pa.
- ASTM. 2012. Standard test method for water content and density of soil in situ by Time Domain Reflectometry (TDR). ASTM standard D6780/D6780M-12. ASTM, West Conshohocken, Pa.
- Bhuyan, H., Scheuermann, A., Bodin, D., and Becker, R. 2017. Use of Time Domain Reflectometry to estimate moisture and density of unbound road materials. *Transportation Research Record: Journal of the Transportation Research Board*, **2655**: 71–81. doi:10.3141/2655-10.
- Briggs, K.M., Loveridge, F.A., and Glendinning, S. 2017. Failures in transport infrastructure embankments. *Engineering Geology*, **219**: 107–117. doi:10.1016/j.enggeo.2016.07.016.
- BSI. 1999a. Compaction-related tests. British standard BS 1377-4. British Standards Institution, London, UK.
- BSI. 1999b. Methods of test for soils for civil engineering purposes. Classification tests. British standard BS 1377-2. British Standards Institution, London, UK.
- BSI. 2015. Code of practice for site investigations. BS5930. British Standards Institution, London, UK.
- Chambers, J.E., Gunn, D.A., Wilkinson, P.B., Meldrum, P.I., Haslam, E., Holyoake, S., et al. 2014. 4D electrical resistivity tomography monitoring of soil moisture dynamics in an operational railway embankment. *Near Surface Geophysics*, **12**(1): 61–72. doi:10.3997/1873-0604.2013002.
- Clarke, B.G., Magee, D., Dimitrova, V., Cohn, A., Du, H., Mahesar, Q., et al. 2017. A decision support system to proactively manage subsurface utilities. In *Proceedings of the International Symposium for Next Generation Infrastructure*. London, UK. Available from <http://eprints.whiterose.ac.uk/120059/>.
- Clayton, C.R.I., Xu, M., Whiter, J.T., Ham, A., and Rust, M. 2010. Stresses in cast-iron pipes due to seasonal shrink-swell of clay soils. *Proceedings of the Institution of Civil Engineers - Water Management*, **163**(3): 157–162. doi:10.1680/wama.2010.163.3.157.
- Curioni, G., Chapman, D.N., Metje, N., Foo, K.Y., and Cross, J.D. 2012. Construction and calibration of a field TDR monitoring station. *Near Surface Geophysics*, **10**(3): 249–261. doi:10.1002/nsg.103001.
- Curioni, G., Chapman, D.N., and Metje, N. 2017. Seasonal variations measured by TDR and GPR on an anthropogenic sandy soil and the implications for utility detection. *Journal of Applied Geophysics*, **141**: 34–46. doi:10.1016/j.jappgeo.2017.01.029.
- Curioni, G., Chapman, D.N., Pring, L.J., Royal, A.C.D., and Metje, N. 2018. Extending TDR capability for measuring soil density and water content for field condition monitoring. *Journal of Geotechnical and Geoenvironmental Engineering*, **144**(2). doi:10.1061/(ASCE)GT.1943-5606.0001792.
- Davies, O., Rouainia, M., Glendinning, S., and Birkinshaw, S.J. 2008. Assessing the influence of climate change on the progressive failure of a railway embankment. In *Proceedings of the 12th International Conference of International Association for Computer Methods and Advances in Geomechanics (IACMAG) 1–6 October, 2008 Goa, India*. pp. 4478–4486.
- Delin, G.N., and Herkelrath, W.N. 2005. Use of soil moisture probes to estimate ground water recharge at an oil spill site. *Journal of the American Water Resources Association*, **41**(6): 1259–1277. doi:10.1111/j.1752-1688.2005.tb03799.x.
- Drnevich, V.P., Ashmawy, A.K., Yu, X., and Sallam, A.M. 2005. Time domain reflectometry for water content and density of soils: study of soil-dependent calibration constants. *Canadian Geotechnical Journal*, **42**(4): 1053–1065. doi:10.1139/t05-047.
- Du, H., Dimitrova, V., Magee, D., Stirling, R., Curioni, G., Reeves, H., et al. 2016. An ontology of soil properties and processes. In *Semantic Web - Iswc 2016, Pt II*. Edited by P. Groth, E. Simperl, A. Gray, M. Sabou, M. Krotzsch, F. Lecue, F. Flock, and Y. Gil. Springer International Publishing Ag, Cham, pp. 30–37.
- Farewell, T.S., Hallett, S.H., Hannam, J.A., and Jones, R.J.A. 2012. Soil impacts on national infrastructure in the United Kingdom. Cranfield University, Cranfield, UK.
- Ferré, P.A., Rudolph, D.L., and Kachanoski, R.G. 1996. Spatial averaging of water content by time domain reflectometry: Implications for twin rod probes with and without dielectric coatings. *Water Resources Research*, **32**(2): 271–279. doi:10.1029/95WR02576.
- Glendinning, S., Hughes, P., Helm, P., Chambers, J., Mendes, J., Gunn, D., Wilkinson, P., and Uhlemann, S. 2014. Construction, management and maintenance of embankments used for road and rail infrastructure: implications of weather induced pore water pressures. *Acta Geotechnica*, **9**(5): 799–816. doi:10.1007/s11440-014-0324-1.
- Glendinning, S., Helm, P.R., Rouainia, M., Stirling, R.A., Asquith, J.D., Hughes, P.N., et al. 2015. Research-informed design, management and maintenance of infrastructure slopes: development of a multi-scalar approach. In *Proceedings of the IOP Conference Series: Earth and Environmental Science*, Vol. 26, Conference 1. doi:10.1088/1755-1315/26/1/012005.
- Gunn, D.A., Chambers, J.E., Uhlemann, S., Wilkinson, P.B., Meldrum, P.I., Dijkstra, T.A., et al. 2015. Moisture monitoring in clay embankments using electrical resistivity tomography. *Construction and Building Materials*, **92**: 82–94. doi:10.1016/j.conbuildmat.2014.06.007.
- Heimovaara, T. 1993. Design of triple-wire time-domain reflectometry probes in practice and theory. *Soil Science Society of America Journal*, **57**(6): 1410–1417. doi:10.2136/sssaj1993.03615995005700060003x.
- Herkelrath, W., Hamburg, S., and Murphy, F. 1991. Automatic, real-time monitoring of soil-moisture in a remote field area with time domain reflectometry. *Water Resources Research*, **27**(5): 857–864. doi:10.1029/91WR00311.
- Hobbs, P., Hallam, J.R., Forster, A., Entwisle, D., Jones, L.D., Cripps, A.C., et al. 2002. Engineering geology of British rocks and soils: mudstones of the Mercia Mudstone Group. RR/01/002. British Geological Survey, Keyworth, Nottingham, UK.
- Janik, G., Dawid, M., Walczak, A., Słowińska-Osypiuk, J., Skierucha, W., Wilczek, A., and Daniel, A. 2017. Application of the TDR technique for the detection of changes in the internal structure of an earthen flood levee. *Journal of Geophysics and Engineering*, **14**(2): 292–302. doi:10.1088/1742-2140/14/2/292.
- Jaroszweski, D., Hooper, E., and Chapman, L. 2014. The impact of climate change on urban transport resilience in a changing world. *Progress in Physical Geography*, **38**(4): 448–463. doi:10.1177/0309133314538741.
- Jung, S., Drnevich, V.P., and Abou, Najm, M.R. 2013a. New methodology for density and water content by time domain reflectometry. *Journal of Geotechnical and Geoenvironmental Engineering*, **139**(5): 659–670. doi:10.1061/(ASCE)GT.1943-5606.0000783.
- Jung, S., Drnevich, V.P., and Abou, Najm, M.R. 2013b. Temperature corrections for time domain reflectometry parameters. *Journal of Geotechnical and Geoenvironmental Engineering*, **139**(5): 671–683. doi:10.1061/(ASCE)GT.1943-5606.0000794.
- Knight, J.H., Ferré, P.A., Rudolph, D.L., and Kachanoski, R.G. 1997. A numerical analysis of the effects of coatings and gaps upon relative dielectric permittivity measurement with time domain reflectometry. *Water Resources Research*, **33**(6): 1455–1460. doi:10.1029/97WR00435.
- Lin, C.P., Siddiqui, S.I., Feng, W., Drnevich, V.P., and Deschamps, R.J. 2000. Quality control of earth fills using Time Domain Reflectometry (TDR). In *Constructing and controlling compaction of earth fills*. ASTM International, West Conshohocken, Pa., pp. 290–310. doi:10.1520/STP15291S.
- Lin, C.-H., Lin, C.-P., and Drnevich, V. 2012. TDR method for compaction quality control: multi evaluation and sources of error. *Geotechnical Testing Journal*, **35**(5): 817–826. doi:10.1520/GTJ104558.
- Met Office. 2018. South West England: climate. Available from <https://www.metoffice.gov.uk/climate/uk/regional-climates/sw> [accessed 23 May 2018].
- National Soil Resources Institute. 2015. Full Soils Site Report for location 350219E, 160072N, 1km x 1km. National Soil Resources Institute, Cranfield University. Available from <https://www.landis.org.uk/sitereporter/>.
- Persson, M., and Berndtsson, R. 1998. Texture and electrical conductivity effects on temperature dependency in time domain reflectometry. *Soil Science Society of America Journal*, **62**(4): 887–893. doi:10.2136/sssaj1998.03615995006200040006x.
- Pritchard, O.G., Hallett, S.H., and Farewell, T.S. 2014. Soil impacts on UK infrastructure: Current and future climate. *Proceedings of the Institution of Civil Engineers: Engineering Sustainability*, **167**(4): 170–184. doi:10.1680/ensu.13.00035.
- Pritchard, O.G., Hallett, S.H., and Farewell, T.S. 2015a. Probabilistic soil moisture projections to assess Great Britain's future clay-related subsidence hazard. *Climatic Change*, **133**(4): 635–650. doi:10.1007/s10584-015-1486-z.
- Pritchard, O.G., Hallett, S.H., and Farewell, T.S. 2015b. Soil geohazard mapping for improved asset management of UK local roads. *Natural Hazards and Earth System Sciences*, **15**(9): 2079–2090. doi:10.5194/nhess-15-2079-2015.
- Rajeev, P., Chan, D., and Kodikara, J. 2012. Ground-atmosphere interaction mod-

- elling for long-term prediction of soil moisture and temperature. *Canadian Geotechnical Journal*, **49**(9): 1059–1073. doi:10.1139/t2012-068.
- Rinaldi, V.A., and Cuestas, G.A. 2002. Ohmic conductivity of a compacted silty clay. *Journal of Geotechnical and Geoenvironmental Engineering*, **128**(10): 824–835. doi:10.1061/(ASCE)1090-0241(2002)128:10(824).
- Robinson, D.A., Jones, S.B., Wraith, J.M., Or, D., and Friedman, S.P. 2003a. A review of advances in dielectric and electrical conductivity measurement in soils using time domain reflectometry. *Vadose Zone Journal*, **2**(4): 444–475. doi:10.2136/vzj2003.4440.
- Robinson, D.A., Schaap, M., Jones, S.B., Friedman, S.P., and Gardner, C.M.K. 2003b. Considerations for improving the accuracy of permittivity measurement using time domain reflectometry: air-water calibration, effects of cable length. *Soil Science Society of America Journal*, **67**(1): 62–70. doi:10.2136/sssaj2003.6200.
- Robinson, D.A., Campbell, C.S., Hopmans, J.W., Hornbuckle, B.K., Jones, S.B., Knight, R., et al. 2008. Soil moisture measurement for ecological and hydrological watershed-scale observatories: a review. *Vadose Zone Journal*, **7**(1): 358–389. doi:10.2136/vzj2007.0143.
- Rosenbalm, D., and Zapata, C.E. 2017. Effect of wetting and drying cycles on the behavior of compacted expansive soils. *Journal of Materials in Civil Engineering*, **29**(1). doi:10.1061/(ASCE)MT.1943-5533.0001689.
- Sadeghioon, A.M., Metje, N., Chapman, D., and Anthony, C. 2018. Water pipeline failure detection using distributed relative pressure and temperature measurements and anomaly detection algorithms. *Urban Water Journal*, **15**(4): 287–295. doi:10.1080/1573062X.2018.1424213.
- Scheuermann, A., Huebner, C., Schlaeger, S., Wagner, N., Becker, R., and Bieberstein, A. 2009. Spatial time domain reflectometry and its application for the measurement of water content distributions along flat ribbon cables in a full-scale levee model. *Water Resources Research*, **45**: W00D24. doi:10.1029/2008WR007073.
- Siddiqui, S.I., and Drnevich, V.P. 1995. Use of time domain reflectometry for determination of water content and density of soil. Joint Highway Research Project, Indiana Department of Transportation and Purdue University, West Lafayette, Indiana. doi:10.5703/1288284313342.
- Siddiqui, S.I., Drnevich, V.P., and Deschamps, R.J. 2000. Time domain reflectometry development for use in geotechnical engineering. *Geotechnical Testing Journal*, **23**(1): 9–20. doi:10.1520/GTJ11119J.
- Stirling, R.A., Glendinning, S., and Davie, C.T. 2017. Modelling the deterioration of the near surface caused by drying induced cracking. *Applied Clay Science*, **146**: 176–185. doi:10.1016/j.clay.2017.06.003.
- Thring, L.M., Boddice, D., Metje, N., Curioni, G., Chapman, D.N., and Pring, L. 2014. Factors affecting soil permittivity and proposals to obtain gravimetric water content from time domain reflectometry measurements. *Canadian Geotechnical Journal*, **51**(11): 1303–1317. doi:10.1139/cgj-2013-0313.
- Topp, G.C., Davis, J.L., and Annan, A.P. 1980. Electromagnetic determination of soil water content: Measurements in coaxial transmission lines. *Water Resources Research*, **16**(3): 574–582. doi:10.1029/WR016i003p00574.
- Utili, S., Castellanza, R., Galli, A., and Sentenac, P. 2015. Novel approach for health monitoring of earthen embankments. *Journal of Geotechnical and Geoenvironmental Engineering*, **141**(3). doi:10.1061/(ASCE)GT.1943-5606.0001215.
- Valentino, R., Montrasio, L., Losi, G.L., and Bittelli, M. 2011. An empirical model for the evaluation of the degree of saturation of shallow soils in relation to rainfalls. *Canadian Geotechnical Journal*, **48**(5): 795–809. doi:10.1139/t10-098.
- Yu, X., and Drnevich, V.P. 2004. Soil water content and dry density by time domain reflectometry. *Journal of Geotechnical and Geoenvironmental Engineering*, **130**(9): 922–934. doi:10.1061/(ASCE)1090-0241(2004)130:9(922).